



Negative Differential Resistance, Instability, and Critical Transition in Lightning Leader

Xueqiang Gou^{1†}, Chao Xin¹, Liwen Xu¹, Ping Yuan¹, Yijun Zhang², Mingli Cheng³

¹ College of Physics and Electronic Engineering, Northwest Normal University, Lanzhou 730070, China

² Department of Atmospheric and Oceanic Sciences & Institute of Atmospheric Sciences, Fudan University, Shanghai, 200438, China

³ Department of Building Environment and Energy Engineering, The Hong Kong Polytechnic University Hong Kong, SAR, China

[†]Corresponding to: Xueqiang Gou (1491168405@qq.com)

Abstract. The phenomena of leader extinction and restrike during lightning events, such as multiple strokes in ground flashes or recoil leaders in cloud flashes, present significant challenges. A key aspect of this issue involves the discussion of the channel's negative differential resistance and its instability. From the perspective of bifurcation theory in nonlinear dynamics, this paper posits an inherent consistency among the channel's negative differential resistance, channel instability, and the critical transition from insulation to conduction. This study examines the differential resistance characteristics of the leader-streamer system in lightning development. We correlate the differential resistance characteristics of the leader-streamer channel with the channel's state and instability transitions, investigating the critical current and potential difference conditions required for the stable transition of the leader-streamer channel.

Key words:

negative differential resistance; instability; critical transition; lightning

1 Introduction

Natural lightning exhibits an intermittent nature distinct from long-gap discharges observed in laboratory settings (Gou et al., 2010; Gou et al., 2018; Iudin et al., 2022). This intermittency is closely related to the fractal and critical characteristics of the lightning process (Bulatov et al., 2020; Sterpka et al., 2021; Iudin & Syssoev, 2022; Syssoev et al., 2022). Additionally, the asymmetry between positive and negative polarities introduces inherent instability in the discharge process, leading to destabilization and re-excitation of lightning events (Van der Velde & Montanya, 2013; Williams, 2016; Williams & Heckman, 2012; Iudin, 2021; da Silva et al., 2023; Scholten et al., 2023).



32 In ground flashes, negative ground flash discharges are typically separated by long
33 intervals of dim light. When the downward negative channel decays and eventually stops, the
34 active intracloud positive part intermittently generates conditions for the formation of dart or
35 dart-stepped leaders (Van der Velde & Montanya, 2013; Stock et al., 2014; Stock et al., 2023;
36 Lapierre et al., 2017; Jensen et al., 2023). In cloud flashes, the active positive leader contrasts
37 sharply with the longer intervals of the negative leader, where K-processes or recoil leaders in
38 the cloud are similar to dart or dart-stepped leaders in negative ground flashes (Van der Velde &
39 Montanya, 2013; Stock et al., 2014; Lapierre et al., 2017).

40 Recoil leaders are generally believed to arise from instability in the bidirectional leader
41 channel due to current interruption (Williams & Heckman, 2012; Mazur, 2016). Stepped leaders
42 are thought to emerge from various instabilities within the streamer channel at the leader's end
43 and their critical transitions (Malagón-Romero & Luque, 2019; Hare et al., 2021). These
44 instabilities often manifest as the negative differential resistance characteristics of the channel.

45 In gas discharge physics, negative differential resistance is typically associated with
46 bistability, hysteresis, and unstable transitions (Bosch & Merlino, 1986; Lozneau et al., 2002;
47 Agop et al., 2012; Raizer & Mokrov, 2013). Since the interaction between the leader and
48 streamer in lightning discharges is inseparable, this paper extends the study of negative
49 differential resistance properties from the leader to the leader-streamer system in lightning. It
50 investigates the stability and instability of the channel during lightning development and the
51 current and potential differences required to maintain channel stability.

52 **2. Method**

53 **2.1 Negative differential resistance in lightning**

54 Lightning, as a natural phenomenon of large-scale arc discharge, exhibits the
55 characteristic of negative differential resistance in its channel (Heckman, 1992; da Silva et al.,
56 2019). This means that as the current increases, the temperature and conductivity of the channel
57 also increases, leading to a further increase in current, while the internal electric field required to
58 maintain the current decreases, and the voltage across the channel decreases. In other words, an
59 increase in current leads to a decrease in voltage, and vice versa ($dV/dI < 0$). Krehbiel et al.
60 (1979) pointed out that the instability of negative differential resistance in the channel might be
61 the main reason for channel attenuation.



62 Heckman (1992) and Williams & Heckman (2012) conducted detailed studies on the
63 relationship between negative differential resistance and the multiplicity of negative ground
64 flashes. They suggested that although the negative differential resistance channel connected to
65 the extended streamer source (which can be considered a current source) is unstable, the
66 existence of resistance and capacitance in the channel itself (both in parallel) forms a stabilizing
67 factor. If the electrical response time constant RC for the channel resistance is greater than the
68 thermal attenuation constant τ of the channel, the channel is stable; otherwise, it is unstable. The
69 critical stability current is approximately 100A (Heckman, 1992; Williams, 2006; Williams &
70 Heckman, 2012).

71 Mazur & Ruhnke (2014) and Mazur (2016a, b) pointed out that equating the leader
72 channel to a parallel arc resistance and capacitance connection might not be appropriate. As the
73 characteristic of the negative effect of channel resistance exists over the entire range of lightning
74 currents, channel stability is not necessarily related to its negative differential resistance
75 characteristics. What determines the stability of the channel is the minimum potential difference
76 condition of the streamer zone at the channel tip (Bazelyan & Raizer, 2000; Mazur, 2016a).
77 Since the initiation and development are guided by a large number of streamers originating from
78 the front, the high resistance of the streamer zone is important for the channel's stability. We
79 suggest that the differential resistance properties of the lightning channel should not only be
80 determined by the leader channel but should also include the streamers at the ends of the leader
81 channel.

82 2.2 Negative differential resistance and bistability

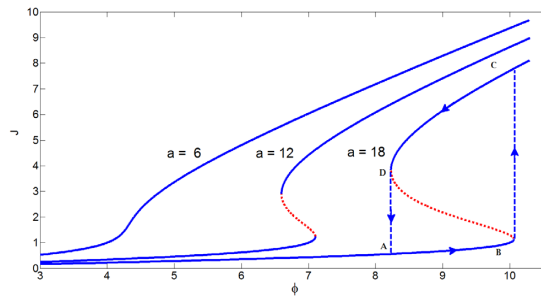
83 Theoretical exploration of negative differential resistance, hysteresis, and bistability led to
84 the derivation of a normalized relationship between current J and voltage ϕ in the discharge
85 channel (Agop et al., 2012):

$$86 \quad \phi = J \left(1 + \frac{a}{1 + J^2} \right) \quad (1)$$

87 Figure 1 shows the theoretical dependence of the normalized current on the normalized
88 voltage. It can be seen that as the parameter a increases, the system changes from stable to
89 unstable. For example, when the parameter $a = 6$, the current monotonically increases with the
90 voltage, and the system is monostable. When the parameter $a = 18$, the system exhibits obvious



91 instability and bistability. Initially, the current increases slowly with the voltage and maintains a
 92 certain state (section AB), but when the voltage reaches a certain limit (point B), the current
 93 suddenly jumps, and the system transitions to a completely different state (point C). When the
 94 voltage begins to decrease in this state, the current decreases with it but maintains a steady state
 95 (section CD). When the voltage decreases to a certain value (point D), the current drops
 96 suddenly, and the system returns to its original state (point A). As the voltage varies, the system
 97 jumps back and forth between two different stable states, thus showing hysteresis, demonstrating
 98 the system's stability, instability and their critical transition under different parameter conditions.



99

100 Fig. 1. Theoretical dependence of the normalized current on the normalized potential (adapted from Agop et
 101 al., 2012, reprinted with permission from the Physical Society of Japan).

102 When examining nonlinear dynamics, it is not uncommon to observe negative differential

103 resistance, bistability, and hysteresis. By considering the dynamic system $\frac{dJ}{dt} = f(\phi, a, J)$,

104 where J is the state variable and ϕ, a is a parameter, we can discern that the system is unstable
 105 when $f(\phi, a, J)=0$ and $f'_J(\phi, a, J) > 0$, conversely, the system achieves stability when

106 $f(\phi, a, J)=0$ and $f'_J(\phi, a, J) < 0$.if we let

107
$$f(\phi, a, J) = \phi - J \left(1 + \frac{a}{1+J^2} \right) \quad (2)$$

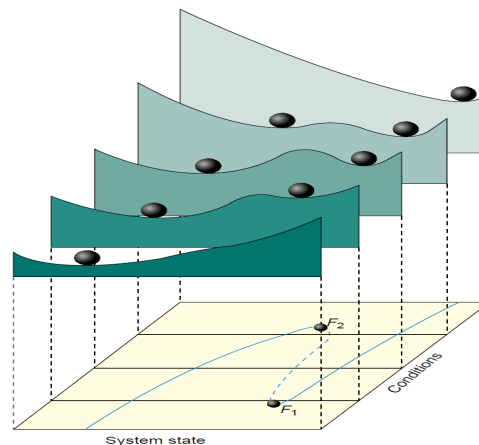
108 then

109
$$f'_J(\phi, a, J) = -1 - a \frac{1-J^2}{(1+J^2)^2} \quad (3)$$



110 Considering equation (1), we have $f'_j(\phi, a, J) = -\phi'(J)$, then the system is unstable
111 under the condition $\phi = J(1 + \frac{a}{1 + J^2})$ and $\phi'(J) < 0$, in agreement with the previous result on
112 the instability of the negative differential resistance. The sign of channel differential resistance
113 provides insight into the stability of channel states and transitions of lightning.

114 Similar bistability, hysteresis, and critical transitions are widely observed in biological,
115 atmospheric, ecological, and other systems and can be described by similar dynamical systems
116 (Scheffer & Carpenter, 2003; Scheffer, 2009). The generation of instability and bistability can be
117 illustrated by the rolling ball model shown in Figure 2, where the peaks and valleys represent
118 unstable and stable points, respectively. Instability triggered by strong nonlinearities (positive
119 feedback) is an important factor causing the bistability (polymorphism) of the system and the
120 critical transition.



121
122 Fig. 2. Schematic representation of the locus of stability as a function of external conditions (adapted from
123 Scheffer & Carpenter, 2003, reprinted with permission from Springer Nature).

124 2.3 The relationship between Lightning channel electric field and current.

125 The measurements of the differential resistance characteristics of a gas discharge gap on a
126 centimeter scale was conducted early by King (1961). However, due to the effect of electrode
127 vaporization as pointed out by Mazur & Ruhnke (2014), King's results can only be applied to
128 currents less than 10A with short gaps. In larger-scale lightning channels, the current and electric
129 field are usually expressed in a power-law form. For instance, Bazelyan et al. (2008) assumed
130 that the leader channel current is inversely proportional to the electric field $E = 3400I^{-1}$, while



131 Larsson et al. (2005) suggested that the relationship between channel current and electric field
 132 varies within the range of 10^2 - 10^4 A

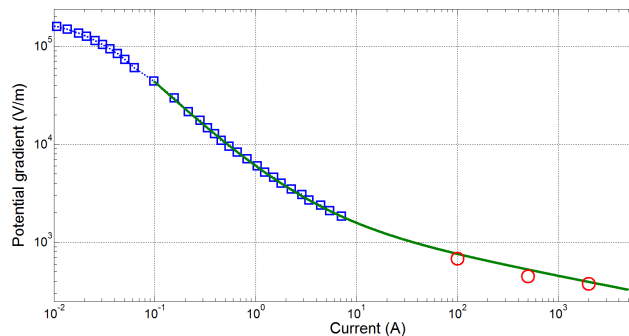
133
$$E = 1600I^{-0.18} \quad (4)$$

134 This is consistent with the observations of Tanaka et al. (2003) and aligns with the
 135 suggestions of da Silva et al. (2019) that the power law differs for each segment within the range
 136 of 10^2 - 10^4 A. To better describe this relationship, we combined the data from King et al. (1961)
 137 and Larsson et al. (2005).

138 For currents less than 10 A, we used the results of King et al. (1961). For currents greater
 139 than 10 A, we applied the formula provided by Larsson et al. (Eq. 4).. Both sets of data were
 140 fitted with a formula.

141
$$E = aI^b + cI^d \quad (5)$$

142 Where $a = 4278$, $b = -0.9788$, $c = 1799$, $d = -0.2006$, the minimum current for
 143 fitting is taken to be approximately 0.1A. Figure 3 shows the relationship between the electric
 144 field and current, where the squares represent King's observations, the circles represent Tanaka's
 145 (2003) experiments, and the solid green line represents the fit.



146
 147

Fig3. electric field versus current in arc channel

148 **2.4 Differential resistance of the leader-streamer channel**

149 A streamer channel's resistance is determined by the potential difference ΔU_T of the
 150 streamer zone of the leader head and the channel current I , which can be expressed as (Bazelyan
 151 & Raizer, 2000)

152
$$I = q_c V_L = 2\pi\epsilon_0 V_L \Delta U_T \quad (6)$$



153 where q_c denotes the channel charge line density and V_L denotes channel development speed, V_L
154 and I follow a power-law relationship (Bazelyan & Raizer, 2000; Popov, 2009)

$$155 \quad V_L = kI^\alpha \quad (7)$$

156 As power exponents vary substantially among studies, for example $\alpha \approx 1/3$ (Hutzler &
157 Hutzler, 1982, Bazelyan et al., 2007), and $\alpha \approx 0.66$ (Kekez & Savic, 1983), in this paper, we
158 adopt $k = 1.88 \times 10^4$, $\alpha = 0.67$ based on more recent studies (Andreev et al., 2008, Popov,
159 2009, Bazelyan et al., 2009).

160 From Eqs. (6) and (7), we obtain the voltage drop in the streamer zone at the leader head

$$161 \quad \Delta U_T = \frac{I}{2\pi\epsilon_0 k I^\alpha} = \frac{I^{1-\alpha}}{2\pi\epsilon_0 k} \quad (8)$$

162 Considering the leader channel potential drop $U_c = LE$, where L is the leader channel
163 length and E is the electric field of the channel as shown in Eq. (4), and the streamer channel
164 potential drop ΔU_T as shown in Eq. (8), the total potential drop U of the leader-streamer system
165 is as follows:

$$166 \quad U = L(aI^b + cI^d) + \frac{I^{1-\alpha}}{2\pi\epsilon_0 k} \quad (9)$$

168 Derive both sides with respect to I gives the total differential resistance

$$169 \quad \frac{dU}{dI} = L(abI^{b-1} + cdI^{d-1}) + (1 - \alpha) \frac{I^{-\alpha}}{2\pi\epsilon_0 k} \quad (10)$$

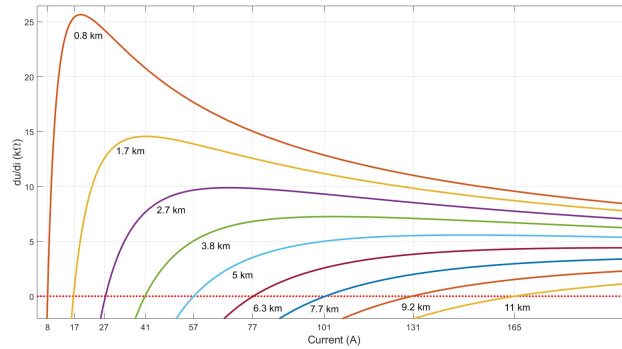
170 3 Analysis results

171 Figure 4 shows how the differential resistance changes as the channel current increases for
172 different lengths of the leader channel, where the horizontal line represents zero differential
173 resistance. When the curve intersects the horizontal line, the differential resistance changes its
174 sign and the horizontal coordinate of the intersection indicates the critical current

175



176
 177
 178
 179
 180
 181
 182
 183

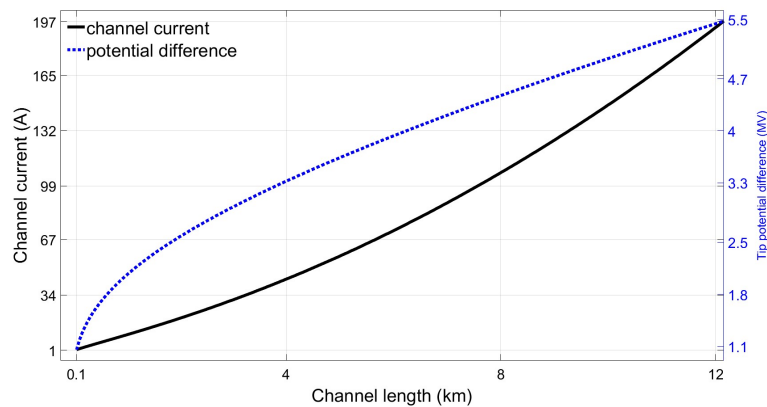


184
 185
 186
 187
 188
 189
 190

Fig4. Dependence of total differential resistance of channel on current with varying channel lengths. The horizontal line represents zero resistance.

191
 192
 193
 194
 195
 196
 197
 198
 199
 200
 201

Figure 5 shows that critical currents increase with channel length, which is consistent with Heckman's 1992 study. It is also shown that the critical potential difference for the streamer zone of the leader's head also increase with leader length, which aligns with the threshold condition for the critical potential difference of the leader's development proposed by Bazelyan & Raizer (2000) and Mazur (2016a).



202
 203
 204

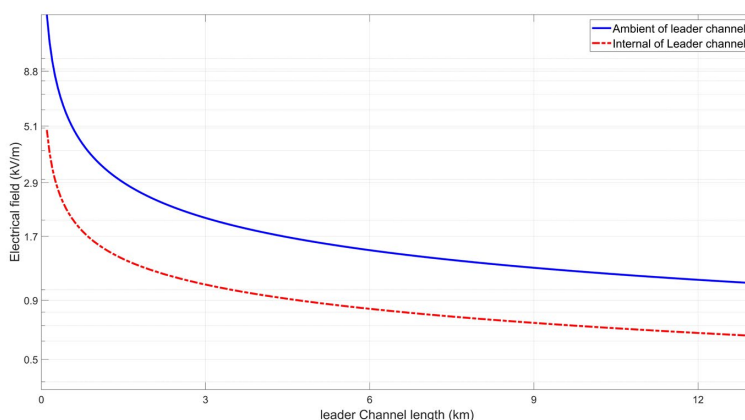
Fig5. Critical channel current and potential difference of the streamer channel at the leader tip vary with channel length.

205
 206
 207

It can be observed that as the leader channel length increases, leader channel's ambient (stabilized) electric field decreases, between 0.1 km and 12 km, the ambient electrical field of the stabilized leader-streamer drops from 15.5 kV/m to 1.1 kV/m, this is consistent with Lalonde et



208 *al. (2002)* and *Becerra & Vernon (2006)* that the leader channel's ambient (stabilized) electric
209 field decreases with the channel's height. Similarly, the internal electric field of the leader
210 channel decreases (Figure 6). At a length of 0.1 km, the electric field is about 4.9 kV/m, while at
211 12 km, it drops to 0.65 kV/m, *Syssoev & Shcherbakov (2001)* determined that stable thermal
212 leader channels with long electric fields (30 – 50 m) were about 3 – 10 kV/m from laboratory
213 discharges, which are also similar to our results.



214
215 Fig 6. variations of ambient electric field of the leader-streamer system and electric field of the leader
216 channels with length

217 4 Discussion and conclusion

218 This paper extends the discussion of lightning discharge channel stability and channel
219 differential resistance from the leader channel to the leader-streamer system. Based on the
220 bifurcation theory and critical transition theory of nonlinear dynamics, the extinction, re-
221 excitation, and critical transition of intermittent events (such as recoil leaders) in the lightning
222 process were studied. By analyzing the sign changes in the differential resistance of the leader-
223 streamer system, the critical current and the critical potential difference in the streamer zone at
224 the channel end were obtained. The results show that as the channel length increases, the critical
225 current of the leader channel and the critical potential difference at the channel end also increase.
226 Meanwhile, the average ambient electric field and the channel electric field required for stable
227 transmission gradually decrease after an initial sharp drop. These findings are qualitatively
228 consistent with existing research results.



229 The specific mechanism behind the sudden change in channel conductivity remains
230 unclear but is undoubtedly related to the instability caused by positive feedback in the channel.
231 The re-excitation of a decayed leader channel is usually due to uneven distribution of current and
232 electric field. The development of a longer channel may exacerbate this inhomogeneity.
233 Typically, the leader head has a higher charge concentration and conductivity, making it more
234 active and persistent, often merging with adjacent channels. In contrast, the rear part of the
235 channel has relatively weaker conductivity and is more prone to disconnection and splitting. This
236 interaction of strength and weakness, merging, and splitting leads to the re-excitation of recoil
237 leaders.

238 In the case of negative ground flashes, the electric field in the upper channel becomes
239 non-uniform due to the low current in the positive leader section, which is insufficient to
240 maintain the conductivity of the lower channel. Recent observations (Williams & Montanya,
241 2019; Hare et al., 2019; Pu & Cummer, 2019; Hare et al., 2021) have found that the low current
242 in the positive leader and the poor conductivity of its corresponding rear leader result in negative
243 charge deposition in the center of the rear channel. This creates a series of outwardly directed
244 negatively polarized needle structures, triggering nonlinear instability. Consequently, the current
245 in the rear part of the positive leader decreases, causing it to disconnect from the negative leader.
246 The increased potential difference at the end of the paused negative leader results in its re-
247 breakdown and reconnection, forming multiple strokes in the negative ground flash process. In
248 the case of positive ground flashes, the upper part of the channel is a negative leader. The
249 stronger current at the head of the negative leader makes the channel less prone to splitting,
250 resulting in a single stroke.

251 The transition from a semiconductor to a conductor state in the leader channel may be due
252 to positive feedback caused by ionization-thermal instability in the channel. As shown in studies
253 by Bazelyan & Raizer (2000), Popov (2009), and da Silva et al. (2019), the pulsed mechanism of
254 the stepped leader is often related to the electric field inhomogeneity among the numerous
255 streamers at the head of the negative leader (Syssoev & Iudin, 2023). The triggering mechanism
256 may be attachment instability (Douglas-Hamilton & Mani, 1974), which exacerbates the
257 inhomogeneity of the electrical properties in the streamer zone (Sigmond, 1984; Luque et al.,
258 2016; Malagón - Romero & Luque, 2019; Malagón Romero, 2021). If the mechanism of the
259 positive stepped leader is similar to that of the negative stepped leader, the stepped excitation



260 should occur in the streamer zone at the leader head (Tran & Rakov, 2016; Kostinskiy et al.,
261 2018; Huang et al., 2020; Wang et al., 2020).

262 Furthermore, whether in the initiation or transmission process, the various
263 inhomogeneities, instabilities, and critical transitions in the leader channel and streamer zone, as
264 well as the emergence of pulse events of different scales and interactions between leader
265 channels, streamers, and various streamers, all exhibit collective, fractal, and critical properties.
266 This may require more unified explanations based on fractal analysis and critical dynamics.

267 **Acknowledgments**

268 The work leading to this paper was supported in part by the National Natural Science
269 Foundation of China (Grant No. 42065005, 42175100 and 42175090) and in part by The Hong
270 Kong Polytechnic University through the Research Grants Council of Hong Kong under Grant
271 GRF15215120

272 **Copyright and Permissions:**We affirm that all third-party copyrighted
273 material used in this manuscript has been obtained with proper permissions.
274 All such material is appropriately cited in the text and captions. Any
275 distribution licenses different from the standard CC BY (Creative Commons
276 Attribution) license are clearly stated below.

277 Figure 1: Adapted from "Experimental and Theoretical Investigations of the
278 Negative Differential Resistance in a Discharge Plasma," by Maricel Agop et
279 al., published in the Journal of the Physical Society of Japan. Used with
280 permission from the Physical Society of Japan. License: Non-commercial use
281 only.

282 Figure 2: Adapted from "Catastrophic regime shifts in ecosystems: linking
283 theory to observation," by Marten Scheffer and Stephen R. Carpenter, published
284 in Trends in Ecology & Evolution. Used with permission from Elsevier. License:
285 CC BY-NC.

286 **Code/Data Availability**

287 The data and code used in this study are available from the corresponding
288 author on reasonable request.

289 **Author Contribution**



- 290 • **Xueqiang Gou**: Conceptualization, Methodology, Software, Validation,
291 Formal analysis, Investigation, Writing – Original Draft, Review &
292 Editing, Visualization, Supervision, Project administration.
293 • **Chao Xin**: Methodology, Software, Formal analysis,
294 • **Liwen Xu**: Visualization.
295 • **Ping Yuan, Yijun Zhang, Mingli Chen**: Conceptualization, Review &
296 Editing Supervision

297 **Competing Interests**

298 The authors declare that they have no known competing financial interests or
299 personal relationships that could have appeared to influence the work reported
300 in this paper.

301 **References**

- 302 Agop, M., P. Nica, O. Niculescu, and D.-G. Dimitriu (2012), Experimental and Theoretical
303 Investigations of the Negative Differential Resistance in a Discharge, *Plasma, Journal of the*
304 *Physical Society of Japan*, 81(6), 064502
- 305 Andreev, A. G., Bazelyan, E. M., Bulatov, M. U., Kuzhekin, I. P., Makalsky, L. M.,
306 Sukharevskij, D. I. and Syssoev, V. S. (2008), Experimental study of the positive leader velocity
307 as a function of the current in the initial and final-jump phases of a spark discharge, *Plasma*
308 *Physics Reports*, 34(7), 609-615, <https://doi.org/10.1134/S1063780X0807009X>
- 309 Bazelyan E, Raizer Y. (2000), *Lightning Physics and Lightning Protection (Bristol: IOP*
310 *Publishing, London)* 27-221
- 311 Bazelyan, E. M., Aleksandrov, N. L., Raizer, Yu P., Konchakov, A. M. (2007), The
312 effect of air density on atmospheric electric fields required for lightning initiation from a long
313 airborne object. *Atmospheric Research* 86(2): 126-138.
- 314 Bazelyan, E. M., Y. P. Raizer, and N. L. Aleksandrov (2008), Corona initiated from
315 grounded objects under thunderstorm conditions and its influence on lightning attachment,
316 *Plasma Sources Science and Technology*, 17(2), 024015
- 317 Bazelyan, E., Syssoev, V., & Andreev, M. (2009). Numerical simulations of spark channels
318 propagating along the ground surface: Comparison with high-current experiment. *Plasma*
319 *Physics Reports*, 35. doi:10.1134/S1063780X0908011X



- 320 Becerra M. and Cooray V. (2006), A simplified physical model to determine the
321 lightning upward connecting leader inception, *IEEE Trans. Power, Delivery*, 21(2), 897–908
- 322 Bosch, R. A., and R. L. Merlino (1986), Sudden Jumps, Hysteresis, and Negative
323 Resistance in an Argon Plasma Discharge. I. Discharges with No Magnetic Field, *Beiträge aus*
324 *der Plasmaphysik*, 26(1), 1-12
- 325 Bulatov, A.A., Iudin, D.I. & Sysoev, A.A. (2020), Self-Organizing Transport Model of a
326 Spark Discharge in a Thunderstorm Cloud. *Radiophys Quantum El* 63, 124–141
327 <https://doi.org/10.1007/s11141-020-10041-z>
- 328 da Silva, C. L., Sonnenfeld, R. G., Edens, H. E., Krehbiel, P. R., Quick, M. G., & Koshak,
329 W. J. (2019), The plasma nature of lightning channels and the resulting nonlinear
330 resistance. *Journal of Geophysical Research: Atmospheres*, 124, 9442–9463.
331 <https://doi.org/10.1029/2019JD030693>
- 332 da Silva, C. L., Winn, W. P., Taylor, M. C., Aulich, G. D., Hunyady, S. J., Eack, K. B.,
333 et al. (2023). Polarity asymmetries in rocket-triggered lightning. *Geophysical Research*
334 *Letters*, 50, e2023GL105041. <https://doi.org/10.1029/2023GL105041>
- 335 Douglas-Hamilton, D. H., and S. A. Mani (1974), Attachment instability in an externally
336 ionized discharge, *J. Appl. Phys.*, 45, 4406, doi:10.1063/1.1663065
- 337 Gou, X., Chen, M., Du, Y., and Dong, W. (2010), Fractal dynamics analysis of the VHF
338 radiation pulses during initial breakdown process of lightning, *Geophysical Research*
339 *Letters*, 37, L11808, doi:10.1029/2010GL043178.
- 340 Gou, X.Q, Chen, M.L, & Zhang, G.S. (2018). Time correlations of lightning flash
341 sequences in thunderstorms revealed by fractal analysis. *Journal of Geophysical Research:*
342 *Atmospheres*, 123. <https://doi.org/10.1002/2017JD027206>
- 343 Gou X. Q, Zhang Y. J, LI Y. J, et al. (2018), Theory and observation of bidirectional leader
344 of lightning: Polarity asymmetry, instability, and intermittency. *Acta Physica Sinica*, 67(20):
345 205201. doi: 10.7498/aps.67.20181079
- 346 Hare, B. M., et al. (2019), Needle-like structures discovered on positively charged lightning
347 branches. *Nature* 568(7752): 360-363
- 348 Hare, B. M., Scholten, O., Dwyer, J., Strepka, C., Buitink, S., Corstanje, A., et al.
349 (2021). Needle propagation and twinkling characteristics. *Journal of Geophysical Research:*
350 *Atmospheres*, 126, e2020JD034252. <https://doi.org/10.1029/2020JD034252>



- 351 Heckman S (1992), Why does a lightning flash have multiple strokes? PhD Thesis
352 Department of Earth, Atmospheric and Planetary Sciences, *Massachusetts Institute of*
353 *Technology*
- 354 Huang, S., Chen, W., Pei, Z., Fu, Z., Wang, L., He, T., et al. (2020), The discharge
355 preceding the intense reillumination in positive leader steps under the slow varying ambient
356 electric field. *Geophysical Research Letters*, 47, e2019GL086183.
357 <https://doi.org/10.1029/2019GL086183>
- 358 Hutzler B and Hutzler D (1982), *EDF Bull. Dir. Etudes Reck.* (serie B) 4 :11-39
- 359 Iudin, D.I., Syssoev, A.A. & Rakov, V. (2022), Problems of Lightning Initiation and
360 Development. *Radiophys Quantum El* 64, 780–803. <https://doi.org/10.1007/s11141-022-10178-z>
- 361 Iudin, D. I., and A. A. Syssoev. (2022), Hot Plasma Channel Network Formation in
362 Thunderclouds. *Journal of Atmospheric and Solar-Terrestrial Physics* 240, 105944.
363 <https://doi.org/https://doi.org/10.1016/j.jastp.2022.105944>.
- 364 Iudin, D. (2021), Lightning as an Asymmetric Branching Network, *Atmospheric Research*
365 <https://doi.org/https://doi.org/10.1016/j.atmosres.2021.105560>.
- 366 Jensen, D., Shao, X. M. and R. Sonnenfeld. (2023), Insights into Lightning K-Leader
367 Initiation and Development from Three Dimensional Broadband Interferometric
368 Observations. *ESS Open Archive* . October 24, DOI: 10.22541/essoar.168275995.55801872/v2
- 369 Kekez M., Savic P. (1983), Correlation leader velocity for current varying from 90 mA to 2
370 kA. *Report 4-th Inter. Symp. On High Voltage Engineering*. Athens, 5-9 Sept. N 45.04.
- 371 King, L. A. (1961), The voltage gradient of the free burning arc in air and nitrogen, *in Proc.*
372 *Fifth Intl. Conference on Ionization Phenomena in Gases*, 2: 871–877, North-Holland, Munich.
- 373 Kostinskiy, A. Y., Syssoev, V. S., Bogatov, N. A., Mareev, E. A., Andreev, M. G., Bulatov,
374 M. U., et al. (2018), Abrupt elongation (stepping) of negative and positive leaders culminating in
375 an intense corona streamer burst: Observations in long sparks and implications for lightning.
376 *Journal of Geophysical Research: Atmospheres*, 123,5360–5375.
377 <https://doi.org/10.1029/2017JD027997>
- 378 Krehbiel, P. R., Brook, M., and McCrory, R. A. (1979), An analysis of the charge structure
379 of lightning discharges to ground, *Journal of Geophysical Research*,, 84(C5): 2432– 2456,
380 [doi:10.1029/JC084iC05p02432](https://doi.org/10.1029/JC084iC05p02432).



- 381 Lapierre, J. L., R. G. Sonnenfeld, M. Stock, P. R. Krehbiel, H. E. Edens, and D. Jensen
382 (2017), Expanding on the relationship between continuing current and in-cloud leader
383 growth, *Journal of Geophysical Research: Atmospheres*, 122, 4150–4164,
384 doi:10.1002/2016JD026189.
- 385 Lalande, P., A. Bondiou-Clergerie; G. Bacchiega; I. Gallimberti et al. (2002). Observations
386 and modeling of lightning leaders, *Comptes Rendus Physique* 3(10): 1375-1392, doi :
387 10.1016/S1631-0705(02)01413-5.
- 388 Larsson, A., A. Delannoy, and P. Lalande (2005), Voltage drop along a lightning channel
389 during strikes to aircraft, *Atmospheric Research*, 76(1), 377-385.
- 390 Lozneau, E., V. Popescu, and M. Sanduloviciu (2002), Negative differential resistance
391 related to self-organization phenomena in a dc gas discharge, *Journal of Applied Physics*, 92(3),
392 1195-1199.
- 393 Luque, A., H. C. Stenbaek-Nielsen, M. G. McHarg, and R. K. Haaland (2016), Sprite beads
394 and glows arising from the attachment instability in streamer channels, *Journal of Geophysical*
395 *Research: Space Physics*, 121, doi:10.1002/2015JA022234
- 396 Malagón-Romero, A., & Luque, A. (2019), Spontaneous emergence of space stems ahead
397 of negative leaders in lightning and long sparks. *Geophysical Research Letters*, 46, 4029–4038,
398 <https://doi.org/10.1029/2019GL082063>
- 399 Malagón Romero, A. F. (2021). Numerical investigation on the advance of leader channels
400 in lightning and long sparks. *Universidad de Granada*.
- 401 Mazur, V., and L. H. Ruhnke (2014), The physical processes of current cutoff in lightning
402 leaders, *Journal of Geophysical Research: Atmospheres*, 119, 2796–2810,
403 doi:10.1002/2013JD020494
- 404 Mazur V. , (2016a) Principles of Lightning Physics (*Bristol: IOP Publishing*) pp1-183
- 405 Mazur, V., (2016b) The physical concept of recoil leader formation, *Journal of*
406 *Electrostatics*, 82:79-87.
- 407 Popov, N. A. (2009), Study of the formation and propagation of a leader channel in air,
408 *Plasma Physics Reports*, 35(9), 785.
- 409 Pu, Y., & Cummer, S. A. (2019). Needles and lightning leader dynamics imaged with 100–
410 200 MHz broadband VHF interferometry. *Geophysical Research Letters*, 46,13556–13563.
411 <https://doi.org/10.1029/2019GL085635>



- 412 Raizer, Y. P., and M. S. Mokrov (2013), Physical mechanisms of self-organization and
413 formation of current patterns in gas discharges of the Townsend and glow types, *Physics of*
414 *Plasmas*, 20(10), 101604.
- 415 Scheffer, M., and S. R. Carpenter (2003), Catastrophic regime shifts in ecosystems: linking
416 theory to observation, *Trends in Ecology & Evolution*, 18(12), 648-656
- 417 Scheffer, M. (2009). *Critical Transitions in Nature and Society (Vol. 16)*. Princeton
418 *University Press*.
- 419 Scholten O, Hare B, Dwyer J, et al. (2023), Searching for intra-cloud positive leaders in
420 VHF. *Research Square*; DOI: 10.21203/rs.3.rs-2631381/v1.
- 421 Sterpka, C., Dwyer, J., Liu, N., Hare, B. M., Scholten, O., Buitink, S., & Nelles, A. (2021).
422 The Spontaneous Nature of Lightning Initiation Revealed. *Geophysical Research Letters*, 48(23),
423 e2021GL095511. <https://doi.org/10.1029/2021GL095511>
- 424 Sigmond, R. S. (1984), The residual streamer channel: Return strokes and secondary
425 streamers, *J. Appl. Phys.*, 56, 1355–1370, doi:10.1063/1.334126
- 426 Stock, M. G., M. Akita, P. R. Krehbiel, W. Rison, H. E. Edens, Z. Kawasaki, and M. A.
427 Stanley (2014), Continuous broadband digital interferometry of lightning using a generalized
428 across-correlation algorithm, *Journal of Geophysical Research: Atmospheres*, 119, 3134–3165,
429 doi:10.1002/2013JD020217
- 430 Stock M, Tilles J, Taylor GB, Dowell J, Liu N. (2023), Lightning Interferometry with the
431 Long Wavelength Array. *Remote Sensing*. 15(14):3657. <https://doi.org/10.3390/rs15143657>
- 432 Syssoev V. S. and Shcherbakov Yu. V., (2001), Electrical strength of ultra-long air gaps, in
433 Proc. 2001 *Int. Conf. on Lightning and Static Electricity*, Seattle, Washington, ID: SAE-2001-01-
434 2898.
- 435 Syssoev, A. A., Iudin, D. I., Iudin, F. D., Klimashov, V. Y., & Emelyanov, A. A. (2022),
436 Relay charge transport in thunderclouds and its role in lightning initiation. *Scientific Reports*,
437 12(1), 1-21. <https://doi.org/10.1038/s41598-022-10722-x>
- 438 Syssoev, A. A., and D. I. Iudin. (2023), Numerical Simulation of Electric Field Distribution
439 inside Streamer Zones of Positive and Negative Lightning Leaders. *Atmospheric Research* 295:
440 107021. <https://doi.org/https://doi.org/10.1016/j.atmosres.2023.107021>.
- 441 Tanaka, S.-I., K.-Y. Sunabe, and Y. Goda (2003), Internal voltage gradient and behavior of
442 column on long-gap DC free arc, *Electrical Engineering in Japan*, 144(3), 8-16



- 443 Tran, M. D., & Rakov, V. A. (2016), Initiation and propagation of cloud-to-ground
444 lightning observed with a high-speed video camera. *Scientific Reports*, 6, 39521.
445 <http://doi.org/10.1038/srep39521>
- 446 Urbani, M., Montanyá, J., Arcanjo, M., & López, J. A. (2022). Multi-Stroke Positive Cloud-
447 To-Ground Lightning Sharing the Same Channel Observed With a VHF Broadband
448 Interferometer. *Geophysical Research Letters*, 49(9), e2021GL097272.
449 <https://doi.org/10.1029/2021GL097272>
- 450 Van der Velde, O. A., and J. Montanya` (2013), Asymmetries in bidirectional leader
451 development of lightning flashes, *Journal of Geophysical Research: Atmospheres*, 118, 13,504–
452 13,519, doi:10.1002/2013JD020257
- 453 Wang, X., Wang, D., He, J., & Takagi, N. (2020), A comparative study on the
454 discontinuous luminosities of two upward lightning leaders with opposite polarities. *Journal of*
455 *Geophysical Research: Atmospheres*, 125, e2020JD032533.
456 <https://doi.org/10.1029/2020JD032533>
- 457 Williams, E.R. (2006), Problems in lightning physics - the role of polarity asymmetry
458 *Plasma Sources Sci. Technol.* 15 (2), S91
- 459 Williams, E. & Heckman, S. (2012), Polarity asymmetry in lightning leaders: The evolution
460 of ideas on lightning behavior from strikes to aircraft. *Aerospace Lab Journal* 5, A105-04, 1–8.
- 461 Williams, E., and J. Montanya (2019), A closer look at lightning reveals needle-like
462 structures, *Nature*, 568, 319–320, doi:10.1038/d41586-019-01178-7.
- 463 Yuan, S., Qie, X., Jiang, R., Wang, D., Sun, Z., Srivastava, A., & Williams,
464 E. (2020), Origin of an uncommon multiple-stroke positive cloud-to-ground lightning flash with
465 different terminations. *Journal of Geophysical Research: Atmospheres*, 125(15),
466 e2019JD032098. <https://doi.org/10.1029/2019jd032098>
- 467 Zhu, Y., Bitzer, P., Rakov, V., Stock, M., Lapierre, J., DiGangi, E., Ding, Z., Medina, B.,
468 Carey, L., & Lang, T. (2021), Multiple Strokes Along the Same Channel to Ground in Positive
469 Lightning Produced by a Supercell. *Geophysical Research Letters*, 48(23), e2021GL096714.
470 <https://doi.org/10.1029/2021GL096714>